# Magnetic properties of ilmenite-hematite solid-solution thin films: Direct observation of antiphase boundaries and their correlation with magnetism

AUTHOR(S):

Hojo, Hajime; Fujita, Koji; Mizoguchi, Teruyasu; Hirao, Kazuyuki; Tanaka, Isao; Tanaka, Katsuhisa; Ikuhara, Yuichi

CITATION:

Hojo, Hajime ...[et al]. Magnetic properties of ilmenite-hematite solid-solution thin films: Direct observation of antiphase boundaries and their correlation with magnetism. PHYSICAL REVIEW B 2009, 80(7): 075414.

ISSUE DATE:

2009-08

URL:

http://hdl.handle.net/2433/109875

PHYSICAL REVIEW B **80**, 075414 (2009)

# Magnetic properties of ilmenite-hematite solid-solution thin films: Direct observation of antiphase boundaries and their correlation with magnetism

Hajime Hojo,[1] Koji Fujita,[2,*] Teruyasu Mizoguchi,[1] Kazuyuki Hirao,[2] Isao Tanaka,[3,4] Katsuhisa Tanaka,[2] and Yuichi Ikuhara[1,4,†]

[1]*Institute of Engineering Innovation, The University of Tokyo, Tokyo 113-8656, Japan*
[2]*Department of Material Chemistry, Kyoto University, Kyoto 615-8510, Japan*
[3]*Department of Material Science and Engineering, Kyoto University, Kyoto 606-8501, Japan*
[4]*Nanostructures Research Laboratory, Japan Fine Ceramics Center, Nagoya 456-8587, Japan*

(Received 21 January 2009; revised manuscript received 28 April 2009; published 11 August 2009)

To clarify the relationship between nanostructures and magnetic properties of $FeTiO_3$-$Fe_2O_3$ solid-solution thin films, we have carried out dark-field transmission electron microscope (DF-TEM) and high-angle annular dark-field (HAADF) scanning transmission electron microscope (STEM) observations. The ordered-phase films show strong ferrimagnetic properties while the films identified as the disordered phase according to x-ray diffraction are weakly ferrimagnetic with high saturation fields, in contrast to completely disordered $FeTiO_3$-$Fe_2O_3$ solid solution for which antiferromagnetic properties or rather small magnetizations are expected. The DF-TEM and HAADF-STEM observations revealed that the ordered-phase films typically consist of cation-ordered domains of over 200 nm and that the Fe and Fe-Ti layers stacked alternately along the *c* axis, which leads to strong ferrimagnetic properties, are clearly distinguishable from each other. On the other hand, the films identified as the disordered phase are found to possess short-range ordered structure with antiphase boundaries distributed in cation-disordered matrix, rather than completely random cation distribution, explaining why the films are weakly ferrimagnetic with high saturation fields. The results demonstrate the significance of atomic-level observation of the cation distribution in this system for understanding the magnetic properties.

DOI: 10.1103/PhysRevB.80.075414 PACS number(s): 61.50.−f, 68.37.Ma, 75.50.Gg, 91.60.Pn

## I. INTRODUCTION

A series of solid solutions between ilmenite ($FeTiO_3$) and hematite ($\alpha$-$Fe_2O_3$) occurs as accessory minerals in igneous and metamorphic rocks and are significant bearers of natural remanent magnetization. Also, members of $FeTiO_3$-$Fe_2O_3$ solid solutions have received revived interest as novel spintronics materials recently[1–7] because of their unique magnetic and electronic properties.[8,9] In this system, the magnetic properties are mainly influenced by two processes: (1) cation ordering in the $FeTiO_3$-rich compositions; (2) exsolution or phase separation in intermediate compositions.[10] Such peculiar properties are considered to originate from an interesting similarity in crystal structures with different symmetry between $FeTiO_3$ and $\alpha$-$Fe_2O_3$.

$FeTiO_3$ has a corundum-type structure, wherein oxide ions form a distorted hexagonal close packing and Fe ions occupy two thirds of the available octahedral interstices forming Fe layers along the *c* axis. $FeTiO_3$ adopts a corundum-derivative structure where Fe layers in $\alpha$-$Fe_2O_3$ are alternately replaced by Ti layers. For their solid solutions, two crystalline phases, i.e., ordered and disordered phases, are generally considered depending on the cation distribution. In the ordered phase, Fe+Ti layers and Fe layers are alternately stacked along the *c* axis. On the other hand, all the cations are randomly distributed in the disordered phase. Ferrimagnetic properties should be observed only in the ordered phase since the negative exchange coupling between adjacent layers usually results in antiferromagnetic properties for the disordered phase.

The ordered phase and disordered phase of $FeTiO_3$-$Fe_2O_3$ solid solution are related to each other via a phase transition in the cation ordering. Upon rapid cooling through the transition temperature, the reduction in symmetry of $R\bar{3}c$ to $R\bar{3}$ often leads to the formation of nanoscale antiphase domains (APDs); each domain is composed of the ordered phase with an alternative sequence of Fe+Ti layers and Fe layers, while adjacent domains are separated by cation-disordered antiphase domain boundaries (APBs). The APBs are generally believed to be responsible for the unusual magnetic properties such as the tendency to acquire the self-reversed thermoremanent magnetization (SR-TRM).[11–13] Namely, the local distribution of Fe and Ti strongly affects the magnetic properties of the solid solutions. Until now, the local cation distribution has been proposed to explain the magnetic anomalies based on conventional transmission electron microscope (TEM) and neutron-diffraction analysis with the aid of computational calculations[10–12,14,15]; however, spatially selective atomic-level observations are required to clarify the unique cation distribution more definitely, especially at the APBs, and also to understand more comprehensively the magnetic properties of this system.

Recent studies on $FeTiO_3$-$Fe_2O_3$ solid-solution thin films have also revealed that the magnetic properties are often inconsistent with those expected from structural analysis using x-ray diffraction (XRD).[2,6,16] For example, Droubay *et al.*[2] have fabricated $x FeTiO_3 \cdot (1-x)Fe_2O_3$ ($x \leq \sim 0.15$) thin films by a molecular-beam epitaxy method and observed nonnegligible magnitude of magnetization for the films characterized as the disordered phase by the XRD pattern. Although the precise atomistic structures are not known, the unusual magnetic properties are presumably associated with the inhomogeneous cation distribution in the crystal. It is not anticipated that detection of the inhomogeneity of cation dis-

 

tribution utilizing XRD is easy because XRD patterns only give spatially averaged information of cation distribution and the difference in x-ray scattering factor between Fe and Ti is small.

On the other hand, recent development of aberration-corrected scanning transmission electron microscopy (STEM) using a high-angle annular dark-field (HAADF) detector achieves a spatial resolution at atomic level for imaging. In a HAADF image, the intensity of each atomic column, that is, a series of atoms aligned along the incident electron-beam direction, is approximately proportional to the square of atomic number, $Z^2$,[17] which generally allows the qualitative interpretation of the images.

In this study, we report on the dark-field transmission electron microscope (DF-TEM) and HAADF-STEM observations for two kinds of $FeTiO_3$-$Fe_2O_3$ solid-solution thin films, which are identified as the ordered and disordered phases by XRD analysis, respectively. Despite the rather small difference in average atomic number between Fe and Fe-Ti columns, we distinctly identified the atomistic structures of these films by the DF-TEM and HAADF-STEM images. Through the observations, we can explain why the films identified as the disordered phase are weakly ferrimagnetic with high saturation fields.

## II. EXPERIMENTAL

Our samples are thin films of solid solutions with compositions of $x FeTiO_3 \cdot (1-x)Fe_2O_3$ ($x=0.6$ and 0.8) epitaxially grown on *c*-plane sapphire (0001) substrates by a pulsed laser deposition method. The thin films with the ordered phase can be obtained by adjusting the oxygen pressure ($P_{O_2}$) and substrate temperature ($T_S$).[18–20] In this study, the ordered-phase thin films were grown under conditions that $P_{O_2}=2.0\times10^{-3}$ Pa and $T_S=700$ °C. For comparison, we also prepared thin film at $P_{O_2}=2.0\times10^{-3}$ Pa and $T_S=600$ °C. After the deposition, all the samples were rapidly cooled to room temperature (cooling rate: 70 °C/min) while keeping $P_{O_2}$ constant. XRD analysis with Cu $K\alpha$ radiation was carried out to identify whether the resultant films were ordered or disordered. Magnetization data were obtained by a superconducting quantum interference device. DF-TEM observations were conducted on a JEOL JEM-2010HC. STEM observations were carried out at room temperature by using JEOL JEM-2100F equipped with a CEOS aberration corrector and a Gatan Enfina electron-energy-loss spectroscopy (EELS) spectrometer. The probe-forming semiangle and EELS detector collection semiangle were around 27 and 23.6 mrad, respectively. Samples for TEM and STEM observations were prepared by mechanical polishing, dimpling, and Ar ion milling so that the electron transparency could be obtained. To minimize the surface damage, the final cleaning was performed by ion milling at 1 kV.

## III. RESULTS AND DISCUSSION

Figure 1(a) displays the XRD patterns of $x FeTiO_3 \cdot (1-x)Fe_2O_3$ ($x=0.6$ and 0.8) solid-solution thin films grown at $T_S=600$ and 700 °C. It is known that 0003 and 0009 diffraction peaks, as well as 0006 and 00012 peaks, are observed for the ordered phase, while the 0003 and 0009 diffraction peaks disappear due to the systematic absence in the disordered phase. For the thin films grown at $T_S=700$ °C, 0003 and 0009 diffraction peaks are present clearly indicative of the formation of ordered phase. Hereafter we will refer to the 0003 and 0009 diffraction peaks as "order peaks". For the thin film grown at $T_S=600$ °C, on the other hand, the absence of the order peaks suggests the formation of disordered phase. Obviously, an increased atomic mobility during the film growth at higher $T_S$ is required to attain the ordered atomic arrangement. Temperature dependence of magnetization of each film is shown in Fig. 1(b). The measurements were performed under field-cooled condition with an external magnetic field of 8500 Oe applied parallel to the film surface. The films of the ordered phase show strong ferrimagnetic behavior as reported earlier.[19,20] Interestingly, the thin film identified as a disordered phase by XRD is also ferromagnetic and possesses high magnetization; it reaches half of the magnetization of ordered phase with the same composition. This behavior is inconsistent with the completely disordered $FeTiO_3$-$Fe_2O_3$ solid solution for which antiferromagnetism or rather small magnetizations is expected. Magnetic field dependence of magnetization measured at 300 K, as shown in Fig. 1(c), gives further insight into the nature of the magnetism for the film without the order peaks. In contrast to the magnetization of the film with the order peaks [closed circles in Fig. 1(c)], the magnetization of the film without the order peaks [open circles in Fig. 1(c)] is not saturated up to high magnetic field. It should also be noted that coercivity at 2 K (not shown) is higher for the film with the order peaks (~2000 Oe) than for the film without the order peaks (~1700 Oe). Such features were often observed in $FeTiO_3$-$Fe_2O_3$ solid solution and linked to the presence of APBs, at which the magnetic domain walls become pinned.[21]

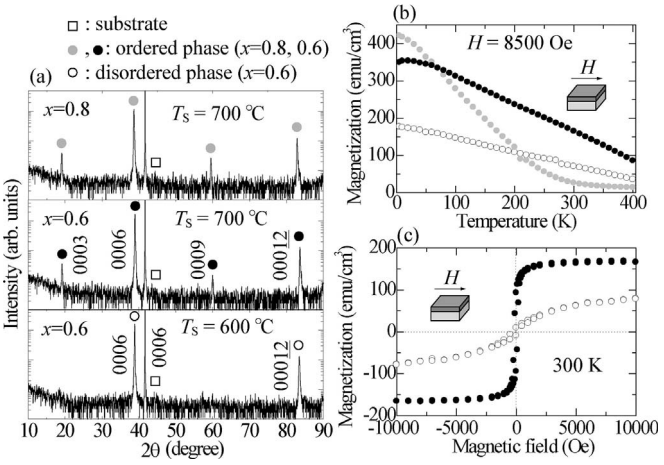


FIG. 1. (a) XRD patterns of $x FeTiO_3$-$(1-x)Fe_2O_3$ [$x=0.6$ (filled circles) and 0.8 (gray circles)] solid-solution thin films prepared under the optimized deposition conditions to obtain the ordered phase ($P_{O_2}$ of $2.0\times10^{-3}$ Pa and $T_S$ of 700 °C) along with the pattern of $0.6FeTiO_3$-$0.4Fe_2O_3$ solid-solution thin film prepared at $T_S$ of 600 °C (open circles). (b) Temperature dependence of magnetization of each film. (c) Magnetic field dependence of magnetization at 300 K.

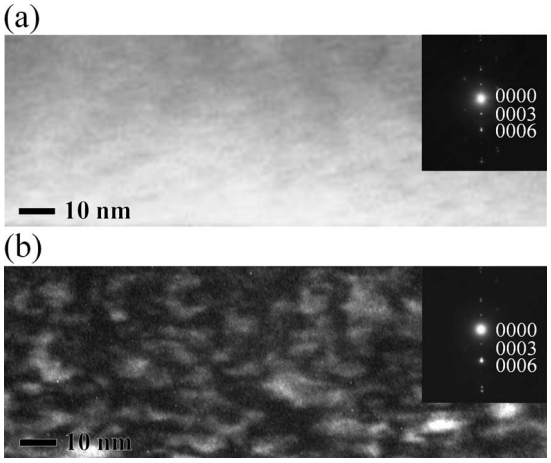


FIG. 2. DF-TEM images of $0.6FeTiO_3 \cdot 0.4Fe_2O_3$ solid-solution thin films (a) with and (b) without the order peaks in XRD pattern. Both of the images were obtained using the ordered 0003 superlattice reflections. The inset of each figure shows selected area electron-diffraction pattern.

Nonsaturating behavior of magnetization has also been reported for $Fe_3O_4$ films grown on MgO substrates, and the modified superexchange interactions at the APBs are suggested to be the origin of such anomaly.[22] Thus, the effect of APBs on the magnetic properties may be significant for the film without the order peaks; however, there are no reports in which one have directly observed the APBs of solid solution at atomic scale and correlated them with the magnetic properties.

To characterize the microstructures of thin films, we have first conducted DF-TEM observations for $0.6FeTiO_3 \cdot 0.4Fe_2O_3$ solid-solution thin films with and without the order peaks in XRD pattern. In DF-TEM images using ordered 0003 superlattice reflections, the ordered and disordered phases show bright and dark contrast, respectively,[11] which allows us to investigate the distribution of cation-ordered domains. The DF-TEM images obtained by use of the ordered 0003 superlattice reflections are displayed in Fig. 2. Since the intensities of ordered 0003 reflections were too weak to form DF images, the sample was tilted by about 5° which enhanced the intensities of 0003 reflections. Here, it should be noted that in contrast to the XRD analysis, the ordered superlattice reflections are clearly observed in the electron-diffraction patterns of both the films (see the inset of Fig. 2). The DF-TEM image of the film with the order peaks in XRD pattern, as shown in Fig. 2(a), indicates the presence of cation-ordered domains over 200 nm in spatial extent meaning that the lateral size of APDs is typically more than 200 nm. As shown in Fig. 2(b), on the other hand, the film without the order peaks in XRD pattern is found to consist of very fine cation-ordered domains of less than 10 nm distributed in cation-disordered matrix rather than separated by APBs. Assuming the size of cation-ordered domains to be 10 nm, the full width at half maximum of 0003 peak in XRD pattern was estimated to be about 0.8° using Scherrer's equation. This value is four times larger than that of 0003 peaks of the films identified as the ordered phase (~0.2° including instrumental broadening) and this fact can be the main reason why 0003 peaks are hard to detect by XRD. The presence of significant amount of cation-disordered phase in our sample seems to be reasonable because the $T_S$ of 600 °C lies in the miscibility gap for the composition of $x=0.6$ in the ilmenite-hematite system.[15] That is, phase separation between Ti-rich ordered phase and Fe-rich disordered phase must occur to some degree during the deposition of the film. Such exsolution reduces the magnetization of the sample depending on the degree of phase separation, as discussed in Ref. 23, because the disordered phase is antiferromagnetic. Moreover, magnetic interactions between the cation-ordered domains need to be considered. When cation-ordered domains are randomly distributed in the cation-disordered matrix, two types of arrangement, in-phase and out-of-phase arrangements, are possible in neighboring domains depending on the relative position of cation layers. In the out-of-phase arrangement, where the position of Fe and Fe-Ti layers are interchanged across the two neighboring domains, negative exchange coupling is expected as in the APBs regardless of the thickness of cation-disordered matrix[13] reducing the magnetization of the sample. Figure 2 clearly demonstrates that the use of only XRD for crystal structural analysis of the solid solutions leads to misunderstanding of the nanostructures. However, the precise atomistic structures of the cation-ordered domains and the interfaces between cation-ordered domains and cation-disordered matrix are hard to determine only by the DF-TEM image. High spatial resolution is necessary to investigate the atomistic structures of the present solid solution.

Thus, in order to identify the cation distribution in the solid solution, atomic-level observations have been performed for the cation-ordered domains using HAADF-STEM. Figure 3(a) shows the HAADF-STEM images of $xFeTiO_3 \cdot (1-x)Fe_2O_3$ ($x=0.6$ and 0.8) solid-solution thin films with the order peaks in the $[11\bar{2}0]$ projection. A projected illustration of the atomic arrangement of the ordered $FeTiO_3$-$Fe_2O_3$ solid solution is also shown in the left side of Fig. 3(a) for direct comparison. Figure 3(b) depicts the intensity profile extracted from Fig. 3(a). Only pairs of atomic columns of cations are visible, while atomic columns for oxide ion have no contrast at all because of too small $Z$. Interestingly, the HAADF signal intensities at the pairs of cation columns exhibit clear systematic variation along the $c$ axis for both thin films with compositions of $x=0.6$ and 0.8. This variation in HAADF signal intensity is ascribable to the presence of the ordered structure, where the positions showing higher and lower intensity correspond to Fe and Fe-Ti columns, respectively. Statistical analysis on several parts of each film has revealed that the average intensity ratios of neighboring brighter and darker columns are $1.11 \sim 1.14$ for $x=0.6$ and $1.22 \sim 1.27$ for $x=0.8$. This result reflects the fact that the Ti ratio in Fe-Ti layers is higher for $x=0.8$ and, hence, the difference in the average $Z$ between Fe layers and Fe+Ti layers is higher for $x=0.8$. To obtain atomistic information, EELS signals were taken for the film of $x=0.6$ with the STEM probe positioned over each pair of atomic columns [0.2 nm × 0.1 nm in size as shown in Fig. 3(a)]. The regions 1 and 2 correspond to the brighter and darker pairs of atomic columns. As expected, a higher Fe signal and a lower

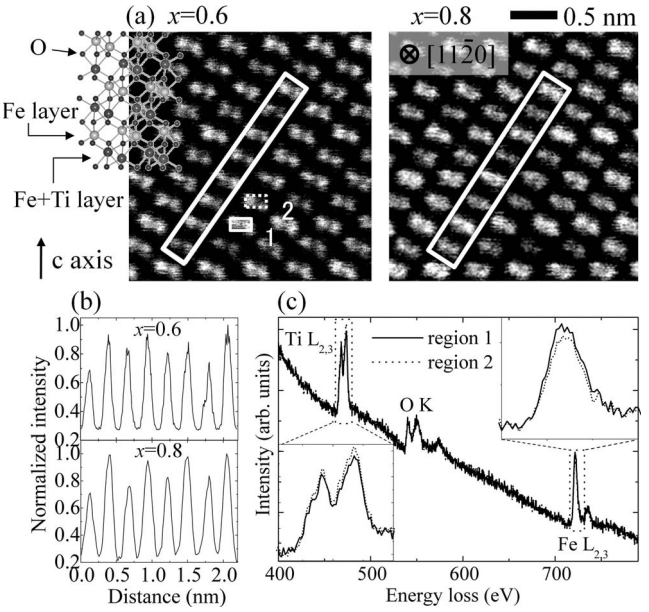


FIG. 3. (a) HAADF-STEM images of $x\mathrm{FeTiO_3}$-$(1-x)\mathrm{Fe_2O_3}$ ($x$ =0.6 and 0.8) in the [11$\bar{2}$0] projection. An illustration of atomic arrangement of the ordered $\mathrm{FeTiO_3}$-$\mathrm{Fe_2O_3}$ solid solution is also shown for direct comparison. Black and gray spheres correspond to cation columns and small black spheres to oxide ion columns. (b) Intensity profiles extracted from the rectangles of white solid line in (a). (c) EELS spectra acquired from the small rectangle of solid line (region 1) and rectangle of dotted line (region 2) in (a).

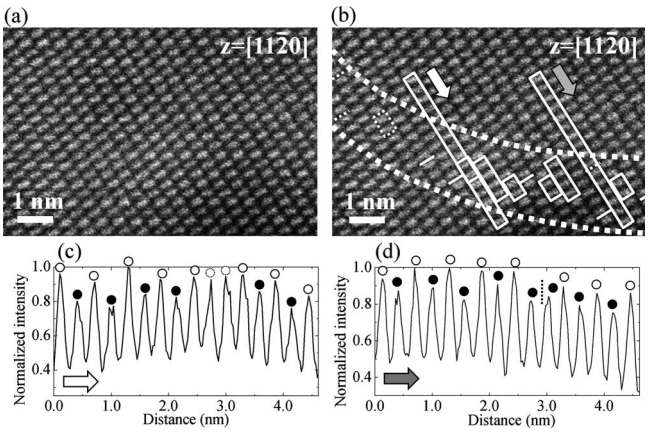


FIG. 4. (a) HAADF-STEM images of $0.6\mathrm{FeTiO_3}$-$0.4\mathrm{Fe_2O_3}$ solid-solution thin film identified as a disordered phase by XRD. (b) Same image with overlay to illustrate the regions where intensity profiles are extracted and a reversal of periodicity in intensity variation occurs. Intensity profiles extracted from long rectangles in (b) are shown in (c) and (d). The regions where the reversal of the periodicity in intensity variation occurs are superimposed on (b) as lines and small rectangles. The boundary is roughly surrounded by thick dotted lines as a guide for the eye.

Ti signal were observed at brighter spot as shown in Fig. 3(c). Compared to the HAADF-STEM image, however, the contrast is much smaller, presumably due to large delocalization in inelastic scattering. Similar EELS spectra were obtained for the films of $x$=0.8. These results demonstrate well that the HAADF-STEM image is powerful to directly investigate cation distribution in the solid solution.

The HAADF-STEM investigation was also performed for $0.6\mathrm{FeTiO_3}\cdot 0.4\mathrm{Fe_2O_3}$ solid-solution thin film without the order peaks in XRD pattern to obtain an insight into the cation distribution inside the cation-ordered domains. Figures 4(a) and 4(b) show the HAADF image of the film and the same image with overlay. Intensity profiles extracted from long rectangles in Fig. 4(b) are illustrated in Figs. 4(c) and 4(d). The ordered structure is clearly observed although the intensity ratio in the ordered region (1.08 ~ 1.11) is slightly lower than that observed in the films with the order peaks (1.11 ~ 1.14). We can also find a region or a boundary where a reversal of the periodicity in intensity variation occurs. In Fig. 4(b), such regions are also surrounded by small rectangles of solid line or dotted line. When the boundaries are clearly defined, they are marked with solid or white dotted lines. Here, the solid and the dotted forms mean that the intensities of columns at the boundary are similar to those of brighter and the darker columns in the APDs, respectively. We can see that there exists a nearly continuous boundary across Fig. 4(b), a so-called APB, which separates cation-ordered APDs. Since each boundary is less than 1 nm in width, it is very difficult to detect such APBs by conventional TEM. The result suggests that the real size of APDs in our sample is smaller than that estimated from DF-TEM images. Harrison *et al.*[14] suggested that when the size of APDs is less than approximately 50 nm, the exchange coupling across APBs is negative in the absence of magnetic wall inside the APDs. This situation is the case with our sample and leads to a further decrease in the magnetization. Furthermore, the slightly lower degree of ordering inside the APDs by itself contributes to the decrease in the order peaks in XRD accompanied by the reduction in the magnetization. Consequently, the anomalous magnetic behavior of the film identified as the disordered phase by XRD is attributable to the presence of cation-ordered domains distributed in cation-disordered matrix as well as the presence of APBs. The x-ray takes it as a disordered phase due to the short-range nature of the cation-ordered domains.

Detailed analysis of intensity profile across the APB provides a new insight into the nature of the APB. Although darker columns are located side by side across the boundary at some parts of the APB [Fig. 4(d)], large part of the atomic columns in the APB are relatively bright with small intensity variations [Fig. 4(c)] indicating that the APB is rich in Fe and possess a disordered cation distribution. Moreover, we can also find that the APB is rather diffuse; the positions where the reversal of the periodicity in intensity variation occurs are scattered in the APB. Such features found in the APB are qualitatively consistent with those predicted by Monte Carlo simulations.[24] However, the interpretation of the HAADF image does not seem so straightforward because the boundary is not always located parallel to the thickness direction. For example, when an APB is tilted, it should give relatively bright region with small intensity variation in a HAADF image. Further systematic experiments should be carried out to explore the nature and distribution of the APBs and their relationship with the magnetic properties such as SR-TRM.

## IV. CONCLUSIONS

In conclusion, we have performed DF-TEM and HAADF-STEM observations on the $FeTiO_3$-$Fe_2O_3$ solid-solution thin films to clarify the relationship between the atomistic structures and the magnetic properties. Despite the rather small difference in average atomic number between Fe and Fe-Ti columns, we successfully observed the ordered structure in the HAADF image and EELS. Interestingly, such ordered structures with an antiphase boundary are also observed in the film identified as a disordered phase by XRD and explain well the magnetic anomalies. These results demonstrate the significance of atomic-level observation for the cation distribution to interpret the magnetic properties of this system. The present experimental techniques will be useful to clarify further curious magnetic properties of the $FeTiO_3$-$Fe_2O_3$ system such as anomalous magnetic properties suggested to stem from unique cation distribution at the interface of nanoscale $FeTiO_3$ and $Fe_2O_3$ exsolution lamellae.[25,26]

## ACKNOWLEDGMENTS

The authors thank H. Jain of Lehigh University, USA for useful discussions. This work was supported by the Grant-in-Aid for Scientific Research on Priority Areas "Nano Materials Science for Atomic-scale Modification" (Grants No. 19053001 and No. 20047008) and also by the Grant-in-Aid for Scientific Research (B) (Grant No. 19360298) from the Ministry of Education, Culture, Sports, Science and Technology (MEXT), Japan. One of the authors (K.F.) acknowledges financial support from the Mizuho Foundation for the Promotion of Sciences, and H.H. is indebted to the Grant-in-Aid (Grant No. 1906281) from the Japan Society for the Promotion of Science (JSPS).

*fujita@dipole7.kuic.kyoto-u.ac.jp
†ikuhara@sigma.t.u-tokyo.ac.jp

[1] W. H. Butler, A. Bandyopadhyay, and R. Srinivasan, J. Appl. Phys. **93**, 7882 (2003).
[2] T. Droubay, K. M. Rosso, S. M. Heald, D. E. McCready, C. M. Wang, and S. A. Chambers, Phys. Rev. B **75**, 104412 (2007).
[3] J. Dou, L. Navarrete, R. Schad, P. Padmini, R. K. Pandey, H. Guo, and A. Gupta, J. Appl. Phys. **103**, 07D117 (2008).
[4] R. Pentcheva and S. N. Hasan, Phys. Rev. B **77**, 172405 (2008).
[5] Y. Takada, M. Nakanishi, T. Fujii, and J. Takada, Appl. Phys. Lett. **92**, 252102 (2008).
[6] H. Ndilimabaka, Y. Dumont, E. Popova, P. Desfonds, F. Jomard, N. Keller, M. Basletic, K. Bouzehouane, M. Bibes, and M. Godlewski, J. Appl. Phys. **103**, 07D137 (2008).
[7] K. Rode, R. D. Gunning, R. G. S. Sofin, M. Venkatesan, J. G. Lunney, J. M. D. Coey, and I. V. Shvets, J. Magn. Magn. Mater. **320**, 3238 (2008).
[8] Y. Ishikawa and S. Akimoto, J. Phys. Soc. Jpn. **12**, 1083 (1957).
[9] Y. Ishikawa, J. Phys. Soc. Jpn. **13**, 37 (1958).
[10] R. J. Harrison, Am. Mineral. **91**, 1006 (2006).
[11] G. L. Nord and C. A. Lawson, Am. Mineral. **74**, 160 (1989).
[12] G. L. Nord, Jr. and C. A. Lawson, J. Geophys. Res. **97**, 10897 (1992).
[13] K. A. Hoffman, J. Geophys. Res. **97**, 10883 (1992).
[14] R. J. Harrison, T. Kasama, T. A. White, E. T. Simpson, and R. E. Dunin-Borkowski, Phys. Rev. Lett. **95**, 268501 (2005).
[15] R. J. Harrison and S. A. T. Redfern, Phys. Chem. Miner. **28**, 399 (2001).
[16] E. Popova, B. Warot-Fonrose, H. Ndilimabaka, M. Bibes, N. Keller, B. Berini, K. Bouzehouane, and Y. Dumont, J. Appl. Phys. **103**, 093909 (2008).
[17] S. J. Pennycook and D. E. Jesson, Ultramicroscopy **37**, 14 (1991).
[18] H. Hojo, K. Fujita, K. Tanaka, and K. Hirao, Appl. Phys. Lett. **89**, 082509 (2006).
[19] H. Hojo, K. Fujita, K. Tanaka, and K. Hirao, Appl. Phys. Lett. **89**, 142503 (2006).
[20] H. Hojo, K. Fujita, K. Tanaka, and K. Hirao, J. Magn. Magn. Mater. **310**, 2105 (2007).
[21] N. E. Brown, A. Navrotsky, G. L. Nord, and S. K. Banerjee, Am. Mineral. **78**, 941 (1993).
[22] D. T. Margulies, F. T. Parker, M. L. Rudee, F. E. Spada, J. N. Chapman, P. R. Aitchison, and A. E. Berkowitz, Phys. Rev. Lett. **79**, 5162 (1997).
[23] R. J. Harrison, S. A. T. Redfern, and R. I. Smith, Am. Mineral. **85**, 194 (2000).
[24] Figure 12(a) in Ref. 10 shows the cation distribution at APDs and APBs formed in a Monte Carlo simulation with $x=0.7$ at $T=850$ K.
[25] P. Robinson, R. J. Harrison, S. A. McEnroe, and R. B. Hargraves, Nature (London) **418**, 517 (2002).
[26] S. A. McEnroe, B. Carter-Stiglitz, R. J. Harrison, P. Robinson, K. Fabian, and C. McCammon, Nat. Nanotechnol. **2**, 631 (2007).